# Measurements of Reactive Recirculating Jet Mixing in a Combustor

Gary D. Smith,* Thomas V. Giel,† and Carl G. Catalano‡
*The University of Tennessee Space Institute, Tullahoma, Tennessee*

**A ducted, subsonic, hydrogen/air turbulent jet mixing flowfield was experimentally investigated, both with and without combustion. The geometric configuration approximated a sudden expansion or "dump" combustor with a central air jet surrounded by a low-velocity hydrogen stream at an overall equivalence ratio of 0.12. The ratio of the duct to inner nozzle diameter was 2.5. Radial distributions of mean axial and radial velocity, axial and radial turbulent intensity, velocity cross correlation, gas composition, static temperature, and total pressure, as well as axial distributions of wall static pressure, were obtained for axial stations 0-6 duct diameters from the combustor entrance. The data indicate that mixing is slower in the chemically reactive flowfield than in the nonreactive flowfield, and that the presence of combustion has a significant effect on the size and location of the recirculation zone within the mixing duct.**

## Nomenclature

$A$ = mass flow rate of air, kg/s
$D$ = duct inner diameter, 13.31 cm
$F$ = mass flow rate of hydrogen, kg/s
$F_H$ = hydrogen mass fraction
$P$ = pressure, N/m$^2$
$R$ = radius, cm
$T$ = temperature, K
$u$ = velocity, m/s
$u'v'$ = velocity cross correlation, m$^2$/s$^2$
$v$ = radial velocity, m/s
$\dot{W}$ = mass flow rate, kg/s
$X$ = axial location from primary nozzle exit, cm
$\Delta p$ = wall static pressure minus wall static pressure at nozzle exit plane, N/m$^2$

*Subscripts*

$c$ = centerline
$D$ = duct
$P$ = primary jet property
$r$ = reference value
$s$ = secondary
$T$ = total or stagnation conditions
$0$ = centerline value at jet exit

*Superscript*

$( )'$ = standard deviation

## Introduction

THE purpose of the study reported herein was to obtain data to aid in the development and evaluation of analytical techniques to analyze and predict the turbulent mixing and combustion phenomena which occur in a wide variety of engineering applications. Development and evaluation of analytical models for ducted, recirculating flow configurations have been hampered by the lack of detailed flowfield measurements for such configurations. This development requires data on different flow configurations if the techniques are to be general and applicable to more than a limited range of parameters. In this study radial distributions of total pressure, mean axial and radial velocity, turbulence intensity, gas composition, velocity cross correlation, and static temperature, as well as wall static pressure distributions were obtained in a confined, axisymmetric, recirculating flowfield typical of a dump combustor. The measurements were obtained both with and without chemical reactions for one fixed stoichiometry at axial stations from 0-6 duct diameters from the combustor entrance. A more detailed description of the investigation together with a complete tabulation of the experimental data can be found in Ref. 1. These data complement data previously obtained in similar flows[2,3] where the duct-to-jet diameter ratio was 10 compared to a diameter ratio of 2.5 in the current apparatus.

The essential features of the recirculating flowfield are shown in Fig. 1. For a certain range of fluid influx conditions, jet mixing of the coaxial streams leads to the creation of an eddy of recirculating fluid which exists on a time-averaged basis as a toroidal, highly vortical region with high turbulent intensities and relatively low average velocities.

## Apparatus

### Test Cell

The test cell, which is a modification of the one used by Schulz[2] and Chriss,[3] is shown in Fig. 2. The test chamber consists of a 1.52 m (5 ft) long stainless steel duct with an inside diameter of 13.31 cm (5.24 in.). A hydraulically driven, axially traversing nozzle assembly mounted inside the duct was traversed in discrete steps during the testing to vary the distance between the primary jet nozzle exit plane and the radially positionable pitot pressure and gas sampling probe. Two O-rings provided a seal between the moveable nozzle assembly and the duct. As is shown in Fig. 2, a 0.635 cm (0.25 in.) wide slot centered at the axial plane of the traversing probe tip provided optical access for the laser instrumentation. A quartz window assembly sealed the slot. Additionally, an optical port, located on top of the test cell in the measuring plane, allowed passage of the pulsed laser beam for the laser Raman system (LRS). An energy dump opposite the optical port dissipated the pulsed laser beam energy.

The primary nozzle assembly consisted of a 5.273 cm (2.076 in.) i.d. circular pipe which introduced the primary air jet at a nominal bulk flow velocity of 102 m/s (335 ft/s). An annular secondary injector assembly provided hydrogen at a nominal bulk velocity of 0.914 m/s (3 ft/s). The secondary hydrogen flow passed through two porous plates and a screen pack,

Presented as Paper 81-1122 at the AIAA 16th Thermophysics Conference, Palo Alto, Calif., June 23-25, 1981; submitted Dec. 8, 1981; revision received May 11, 1982. 

*Facility Manager, Energy Conversion R&D Programs (ECP). Member AIAA.
†Supervisor, Advanced Measurements Group, ECP. Member AIAA.
‡Project Engineer, Fuels and Combustion Group, ECP.

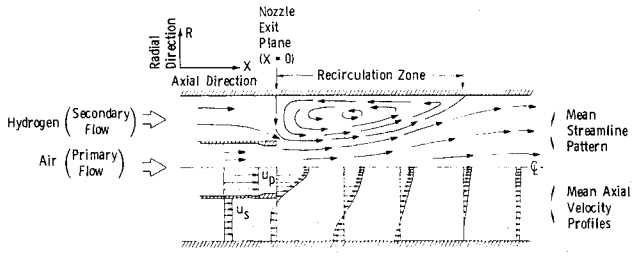


**Fig. 1 Ducted, recirculating flowfield.**

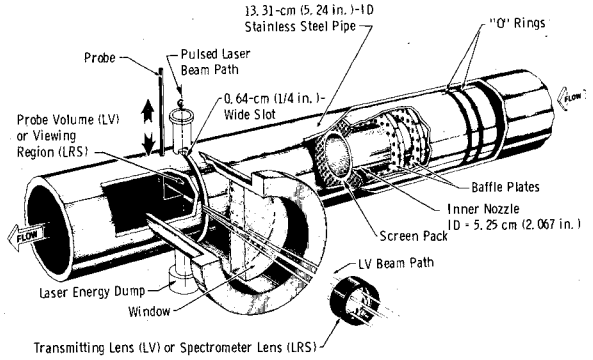


**Fig. 2 Recirculating flow combustor.**

shown in Fig. 2, to establish a reasonably uniform secondary flow. External water spray nozzles were positioned outside the duct to cool the walls. A spark plug was located downstream of the traversing probe to ignite the combustible hydrogen/air mixture.

### Instrumentation

*Pressure and Temperature*

A water-cooled total pressure and gas sampling probe of the type described in Ref. 4 was installed in the duct. By changing the positions of the axially traversing nozzle assembly and the radially traversing probe, axial and radial surveys were made in the recirculating flowfield. The total pressure was sensed with both a variable capacitance transducer and a strain gage transducer to obtain maximum accuracy over the range of pressure encountered.

In addition to the probe assembly, 41 static pressure orifices 0.102 cm (0.040 in.) in diameter were installed approximately 2.54 cm (1 in.) apart along the duct wall. The orifices were connected to a water manometer which was photographed during the tests to record the wall static pressure distribution.

The total temperature of the gaseous supplies of hydrogen and air were measured with copper-constantan thermocouples located upstream of critical flow venturis, which were used to measure the primary and secondary supply flows.

*Gas Concentration*

The mass fraction of hydrogen present in the probe-extracted gas samples was measured using two different techniques. Gas samples from the nonreactive tests were analyzed with a thermal conductivity cell apparatus similar to that described in Ref. 5. The cell was calibrated prior to each test period with known mixtures of $GH_2/GN_2$. Gas samples from the reactive tests were analyzed using an infrared emission/absorption apparatus similar to that described in Ref. 6. Prior to analysis, reactive gas samples passed through a platinum-wound catalytic heater to insure completion of the chemical reaction. Since the emission/absorption system measured water vapor mass fraction, the entire gas sampling system was steam heated to prevent water vapor condensation.

Additionally, for the case of flow with chemical reactions, species concentrations and static temperatures were measured using an in situ laser Raman spectroscopy apparatus which is described in detail in Ref. 7. The Q-switched ruby laser beam was transmitted vertically through the test cell so that the spectrometer could collect the stronger Raman scattering perpendicular to the laser beam. The resulting measurement volume was 0.99 mm (0.039 in.) in diameter by 0.318 cm (0.125 in.) long. Temperature and air number density were determined by measuring the intensity of the $N_2/O_2$ rotational Raman lines as described in Ref. 7. The laser pulse width was 20 ns, and the repetition rate was 15 pulses/min. Only 15 pulses were obtained per data point, resulting in a relatively broad statistical confidence interval.[8] For a 95% confidence level the mean temperatures in the recirculating eddy have a confidence interval of nearly 20%. The results obtained for the mean temperature and species number density are, therefore, only approximations to the true values of these parameters.

### Velocity and Turbulence

Axial and radial velocities were measured in the duct with the individual realization laser velocimeter. A Bragg-diffracted system, as described in Ref. 9, was used both to distinguish the two velocity components and to measure the flow directionality. The 514.5 nm wavelength line from an argon-ion laser was split by the Bragg cell and the four lowest order beams were directed and focused to a measuring region or probe volume in the flowfield. Particles passing through the probe volume scatter light which is analyzed to determine the particle velocity and direction for the axial and vertical coordinates. Scattered light is collected in the backscatter direction to simplify optical access and traversing arrangements. Off-axis collection was used to reduce the probe volume size to an approximate cylinder of 0.3 mm diam and 1.2 mm length. Generally, measurements were restricted to about 1500 simultaneous measurements of both axial and radial components so that mean turbulent intensities and the $u'v'$ correlation could be determined concurrently[10] with a reasonable statistical confidence. The system has the capability to measure velocities over an axial velocity range $-75 \le U \le 215$ m/s ($-250 \le U \le 700$ ft/s) and a vertical velocity range $-75 \le V \le 75$ m/s ($-250 \le V \le 250$ ft/s).

At the temperatures in the chemically reacting flowfield, not enough natural particles survive to obtain velocity measurements within a reasonable time period. A particle seeding device was developed with which the primary airstream was seeded with uniform 1-$\mu$m-diam alumina particles. A discussion of seeding effects and statistical bias errors are given in Ref. 1, as well as a detailed discussion of test procedures. Additional details of the laser Raman procedures are given in Ref. 7. Measurement uncertainties, presented in Table 1, were obtained with techniques described in Ref. 1.

## Results and Discussion

Experimental data were obtained for both reactive and nonreactive flow. A complete tabulation of the experimental data is presented in Ref. 1. The nominal test conditions are presented in Table 2. The fully mixed temperatures were nominally 291 K (65°F) for the nonreactive case and 977 K (1300°F) for the reactive case (assuming chemical equilibrium and negligible wall heat transfer).

### Pressure Measurements

The axial distribution of wall static pressures is shown in Fig. 3. The pressure distributions clearly indicate that one significant effect which the chemical heat release has on the recirculating flowfield is to change the rate of wall static pressure rise. The radial distributions of total pressure are shown in Figs. 4 and 5. A comparison of Figs. 4 and 5,

**Table 1 Measurement uncertainties**

| Parameter | Representative value of parameter | Uncertainty,[a] % of value |
|---|---|---|
| Wall static pressure | 273 N/m$^2$ (0.04 psig) | ±5.0 |
| Probe pitot pressure | 20.7 kN/m$^2$ (3 psig) | ±2.0 |
| LV measured axial velocity | 91.4 m/s (300 ft/s) | ±3.0 |
| | −30.5 m/s (−100 ft/s) | ±4.0 |
| LV measured radial velocity | 9.14 m/s (30 ft/s) | ±3.5 |
| | 3.05 m/s (10 ft/s) | ±8.0 |
| Hydrogen mass fraction (nonreacting) | 0.03 | ±5.0 |
| Hydrogen mass fraction (reacting) | 0.04 | ±16.0 |
| Primary air mass flow | 0.263 kg/s (0.580 lbm/s) | ±2.0 |
| Secondary hydrogen mass flow | 0.00071 kg/s (0.002 lbm/s) | ±6.0 |
| Probe radial position | 7.62 cm (3 in.) | ±6.2 |
| Probe axial position | 76.2 cm (30 in.) | ±1.4 |
| Laser Raman measured temperature | 1111 K (2000 °R) | ±10.0 |

[a] Uncertainty determined from the technique detailed in Ref. 1.

**Table 2 Nominal test conditions**

| Parameter | Nominal value |
|---|---|
| $F/A$ | 0.00345 kg $H_2$/kg air |
| $\dot{W}$ (air) | 0.263 kg/s (0.580 lbm/s) |
| $\dot{W}$ ($H_2$) | 0.0009 kg/s (0.002 lbm/s) |
| $P$ (exhaust) | 94.4 kN/m$^2$ (13.7 psia) |
| $T_T$ (air) | 289 K (520 °R) |
| $T_T$ ($H_2$) | 311 K (560 °R) |
| $u$ (air) | 102 m/s (335 ft/s) |
| $u$ ($H_2$) | 0.914 m/s (3 ft/s) |

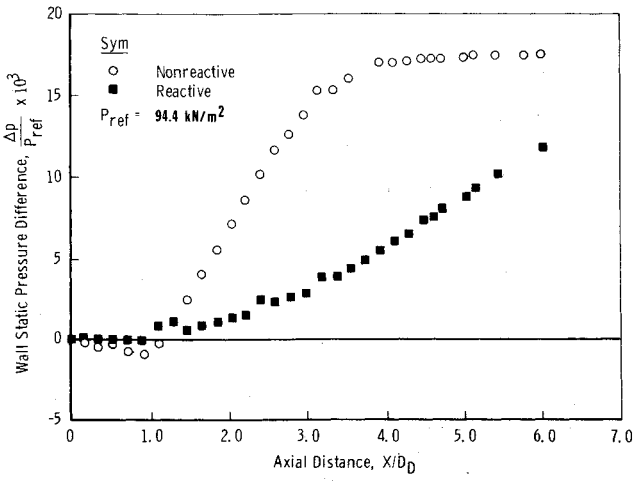


**Fig. 3 Axial distribution of wall static pressure.**

particularly for $X/D$ greater than 2, reveals that the total pressure decay is slowed by the chemical heat addition, indicating that the effect of the chemical reaction is to reduce the rate of momentum transport between the two coaxial streams. The shape of the total pressure profiles also demonstrates the reduced mixing rates.

### Laser Velocimeter Measurements

Representative radial distributions of mean axial velocity, mean radial velocity, axial turbulence intensity, radial turbulence intensity, and the velocity cross correlation are shown in Figs. 6-10 both with and without chemical reaction. The velocity data are nondimensionalized by the one-dimensional primary jet flow velocity $u_p$ and the axial and radial distances are ratioed to the duct diameter and radius, respectively. Data are presented for three representative axial locations.

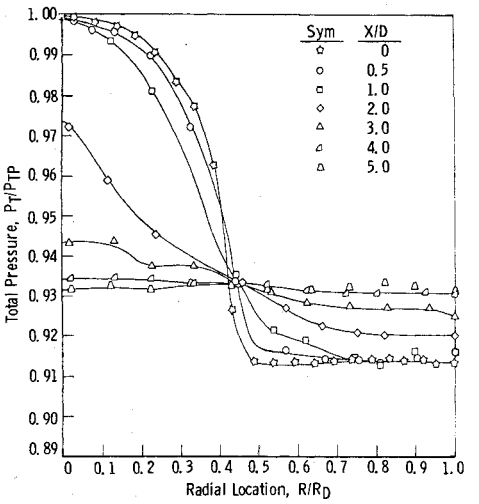


**Fig. 4 Radial distribution of total pressure in nonreacting flow.**

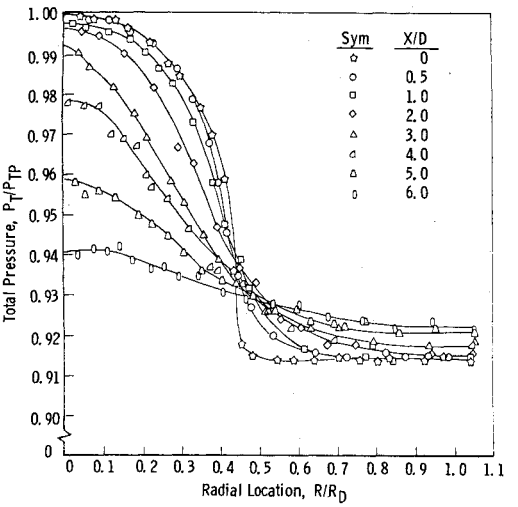


**Fig. 5 Radial distribution of total pressure in reacting flow.**

It should be noted that only the center jet flow was seeded with alumina particles. Since the outer jet bulk velocity was low, it was thought that if only the center jet were seeded, the recirculation eddy would act to distribute the seed material throughout the flow and this did occur for the nonreactive case. However, for the reactive case, the alumina deposited on the walls and as a result the recirculation eddy did not

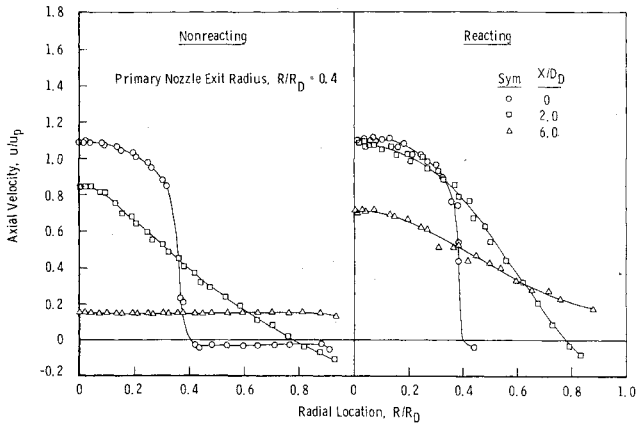


**Fig. 6 Radial distribution of mean axial velocity.**

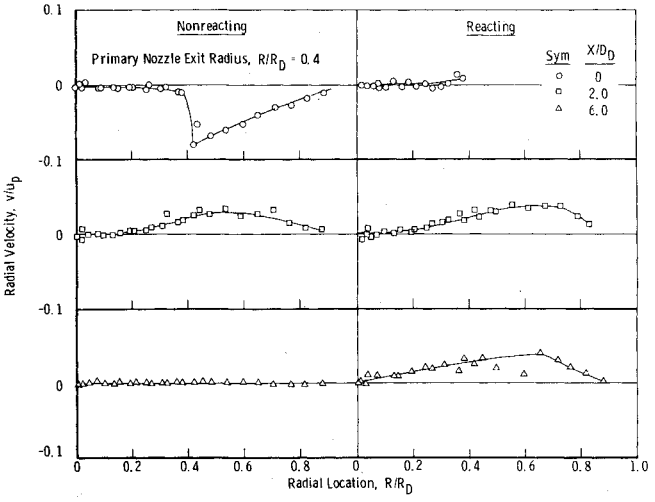


**Fig. 7 Radial distribution of mean radial velocity.**

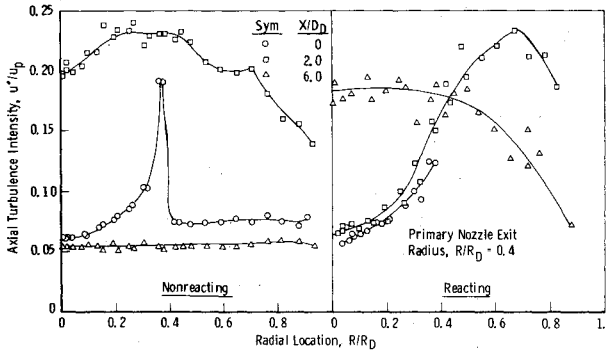


**Fig. 8 Radial distribution of axial turbulence intensity.**

distribute sufficient seeding material across the outer stream in the region near the primary nozzle exit plane. Therefore, velocity measurements could not be obtained in the flow near the duct wall in a reasonable sampling time.

The data presented in Figs. 6-10 show radial profiles of velocities both with and without chemical reactions to demonstrate the effects of the chemical heat release. It is evident from the mean axial velocity variation (Fig. 6) that chemical heat addition broadens the profile and reduces the axial velocity decay. The profiles of radial velocity (Fig. 7) also indicate, although less dramatically, the sustained high axial core velocity resulting from the chemical reaction. The maximum values of both turbulence intensities, $u'/u_p$ and $v'/u_p$ (Figs. 8 and 9), are about the same with or without

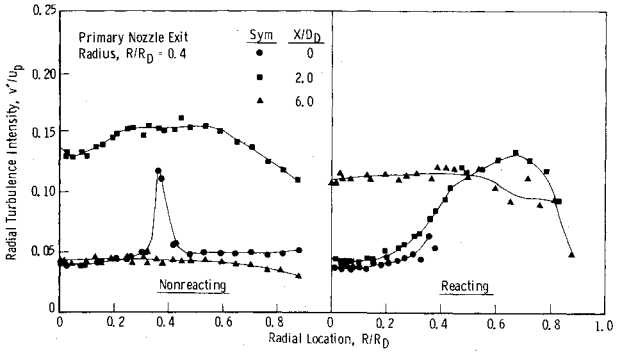


**Fig. 9 Radial distribution of radial turbulence intensity.**

reaction. However, the axial location of the maximum turbulence intensity (not shown) is reached closer to the primary nozzle exit plane in the nonreacting case because in each case the location of the maximum turbulence intensity occurs near the midpoint of the length of the mixing zone, which extends farther downstream with chemical reaction. The turbulence intensity becomes essentially constant by $X/D=4$ for the nonreactive case, whereas significant nonuniformity still exists at $X/D=6$ for the reactive case. Note by comparing the data in Figs. 7 and 9 that the magnitude of the radial rms velocity fluctuations is much greater than the mean radial velocity at nearly every point in the flowfield. The velocity cross correlation $u'v'/u_p^2$ shown in Fig. 10 also indicates a considerable effect of chemical heat release on the Reynolds stress field.

The decay of the mean axial velocity along the duct centerline is shown in Fig. 11. As implied from the previously presented data, the measurements reveal that the velocity decays less rapidly in the reactive case than in the nonreactive case. This result is consistent with results presented in Ref. 3, but a complete explanation for this phenomenon has not been given. It is recognized that, for constant area duct flow with mixing and heat addition, the average velocity in the duct must be higher for the reactive case for the same pressure and mass flow because of the higher temperature. However, the reason for the delayed decay of the potential core region in the reactive case, where neither mixing nor burning has taken place, is not obvious.

Figure 12 shows the location of the locus of points of zero mean axial velocity in the recirculation flowfield, both reactive and nonreactive. Note that the locus does not represent the dividing streamline and in fact corresponds to the dividing streamline at only two points, the forward and rear duct wall stagnation points (Fig. 1). Figure 12 clearly demonstrates the effect of the chemical heat release on the location and extent of the recirculation zone. The downstream reattachment point lies between $X/D=3$ and 4 for the nonreactive case and near $X/D=6$ for the reactive case. The result is significantly different from the results obtained by Schulz[2] and Chriss[3] on a similar configuration but with a mixing duct to primary jet diameter ratio of 10.0 rather than the present diameter ratio of 2.5.

The radial distributions of elemental hydrogen mass fraction $F_H$ for the nonreactive case are shown in Fig. 13. Because of the mixing process, the centerline value of $F_H$ increases and the near-wall value decreases with increasing axial distance from the primary nozzle exit plane. Note that no pure hydrogen was measured, even close to the exit plane. This was expected since the velocity data indicate that the recirculation zone extends nearly all the way back to the exit plane. In addition, the low values of $F_H$ and the highly turbulent velocity field near the wall indicate that counterstream turbulent diffusion of species apparently caused dilution of the hydrogen stream. This result is consistent with the results of Chriss[3] for the diameter ratio 10 configuration.

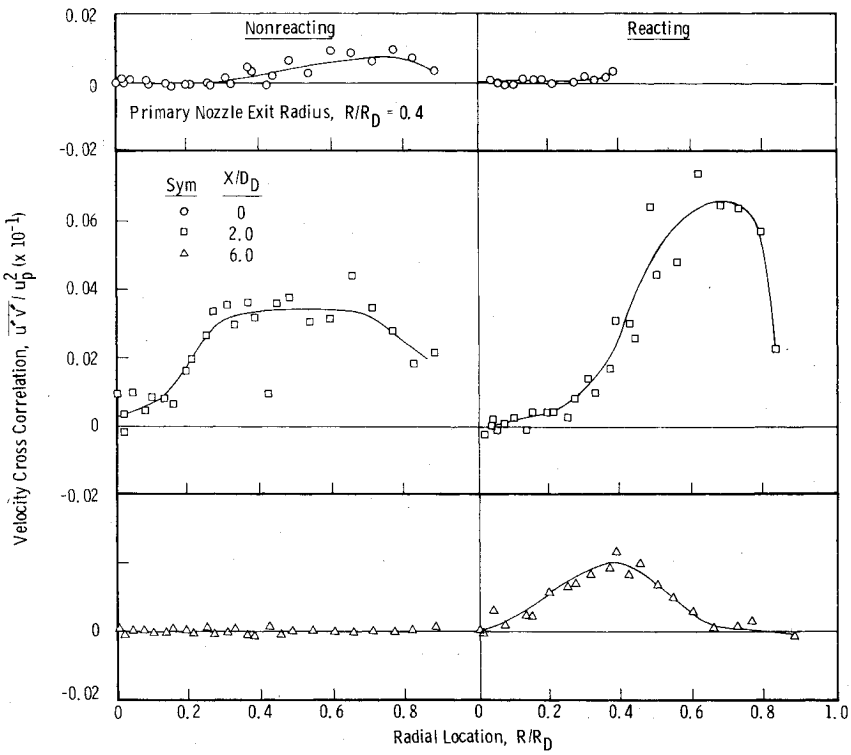


Fig. 10 Radial distribution of velocity cross correlation.

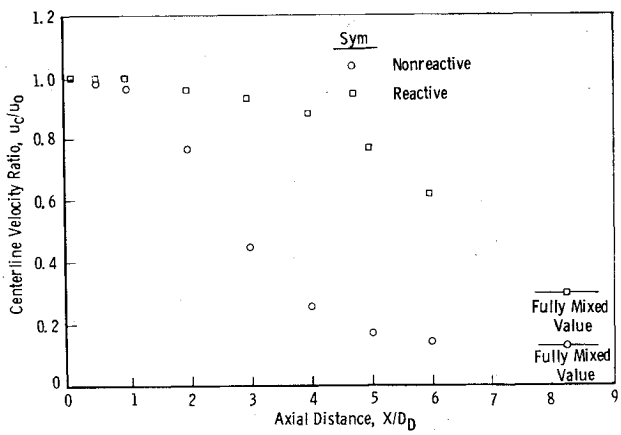


Fig. 11 Axial distribution of mean centerline axial velocity.

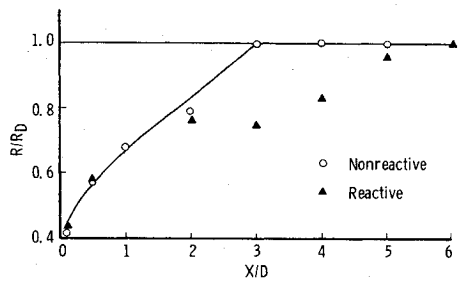


Fig. 12 Locus of zero mean axial velocity (diameter ratio 2.5).

The radial distributions of $F_H$ for the reactive case are shown in Fig. 14. As before, the centerline value of $F_H$ increases and the wall value decreases with increasing axial distance from the primary nozzle exit plane, and no pure hydrogen was measured in the flowfield. However, the data indicate that the mixing is less rapid in the reactive than in the nonreactive case, causing the dilution of the hydrogen stream to be less rapid.

The axial distribution of $F_H$ along the mixing duct wall is presented in Fig. 15 for both the reactive and nonreactive cases. The data show that $F_H$ decays less rapidly in the reactive case, indicating more rapid mixing in the nonreactive flowfield, which is consistent with the previously presented data. The nonreactive $F_H$ decays to the fully mixed value by $X/D=6$ while for the reactive case mixing is not complete at this station. The data also indicate that the upstream diffusion of species extends to the primary nozzle exit plane since $F_H$ is less than unity in this region.

### Laser Raman Measurements

Radial distributions of mean static temperature are presented in Fig. 16 for five axial locations in the recirculating, reacting flowfield. The mean temperatures were obtained by calculating a value of temperature for each of the 15 samples measured per data point and then arithmetically averaging to obtain a "mean" value. The temperature distributions, as expected, show that the temperature is low on the centerline in the near field and increases with radial distance toward the duct wall to some peak value in the turbulent recirculation zone. The radial temperature distribution in the far field ($X/D=6$) is relatively flat at a level consistent with the fully mixed fuel/air ratio when the heat loss to the cooled duct wall is considered.

Mean temperatures at the level of stoichiometric hydrogen/air combustion (2300 K) were not measured anywhere in the flowfield. However, examination of a typical set of 15 samples of temperatures (Fig. 17) shows that in the near field ($X/D=1$) instantaneous values of approximately stoichiometric flame temperature did exist. The number of samples obtained was not sufficient to define the statistical behavior; nevertheless, the 15 points clearly show huge temporal fluctuations in temperature (and hence concentration) in the near field with a mean value of 1411 K and fluctuations between 700 and 2300 K (stoichiometric). Temperatures measured in the far field ($X/D=6$) where the flow approaches being fully mixed, are also presented in Fig. 17 and the temperature fluctuations are much smaller. The implications of the initially large temporal fluctuations of temperature and concentration on the mean flow properties

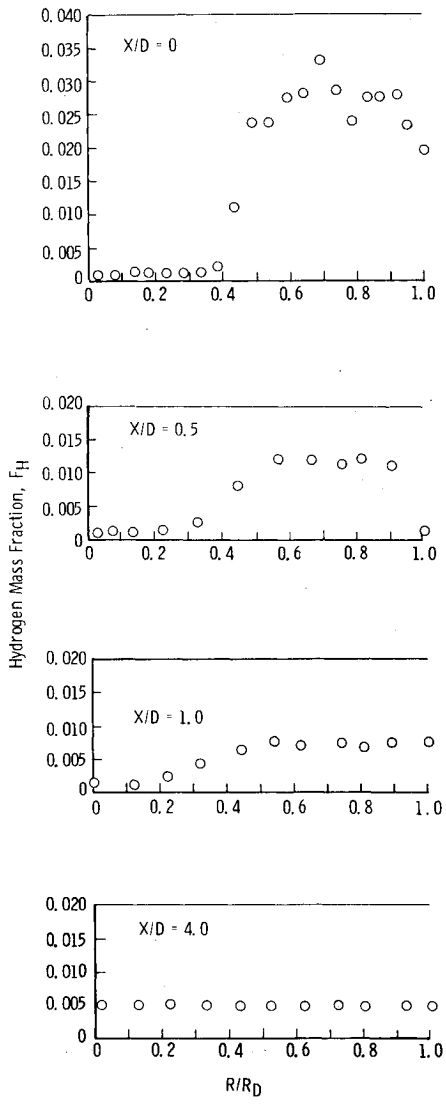


**Fig. 13 Radial distribution of $H_2$ mass fraction in nonreacting flow.**

and the reaction kinetics are such that the generally satisfactory prediction of the details of reaction kinetics in such combustor flows must account for the existence of the huge fluctuations.[11]

## Conclusions

Ducted, hydrogen/air, nonreacting and reacting, recirculating flow experiments were conducted in a combustor with a ratio of duct to inner nozzle diameter of 2.5. Analysis of the data leads to the following conclusions:

1) The size and location of the recirculation zone are appreciably altered by the presence of chemical reactions. This is indicated by differences in the locus of zero mean velocity locations in the recirculating zone and in the wall static pressure distributions for the reactive and nonreactive cases. This result is very different from the result obtained in the diameter ratio 10 configuration.[3] The clear implication of this result is that the historical approach of modelling combustor flows by cold-flow testing techniques is not always satisfactory and hot-flow testing is required to verify designs.

2) The gases in a ducted, axisymmetric, reacting, recirculating flow mix more slowly than those in a nonreactive system of the same configuration and fuel/air ratio. The decay of concentration and velocity is less rapid, and the radial distributions of concentration and velocity approach uniform profiles less rapidly for the reacting case.

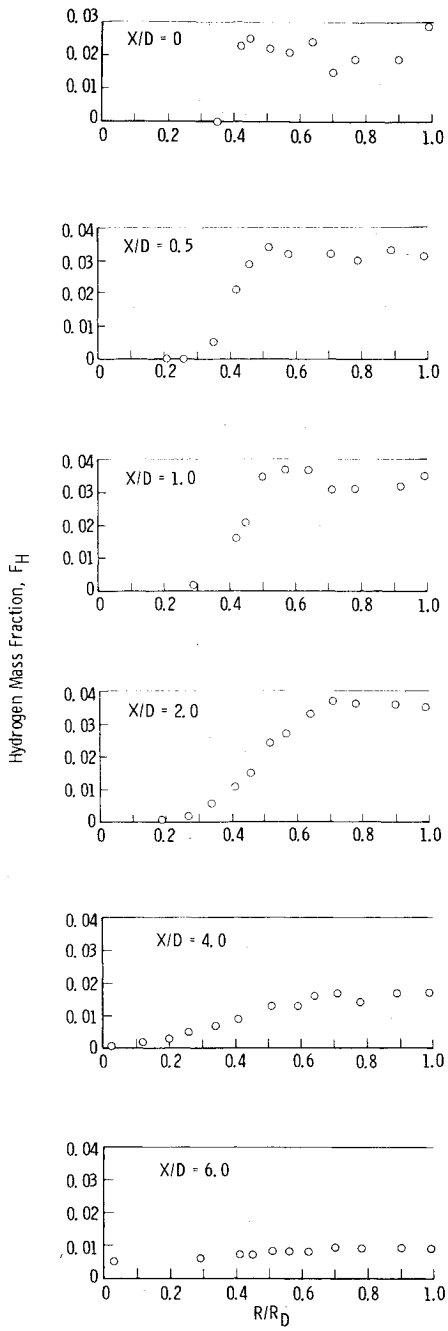


**Fig. 14 Radial distribution of $H_2$ mass fraction in reacting flow.**

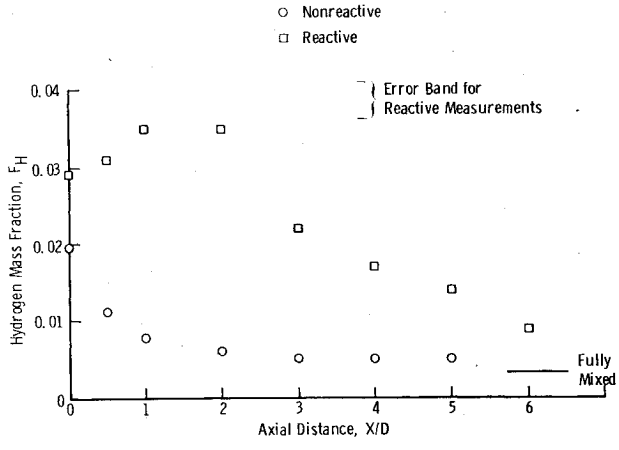


**Fig. 15 Axial decay of $H_2$ mass fraction at $R/R_D = 1.0$.**

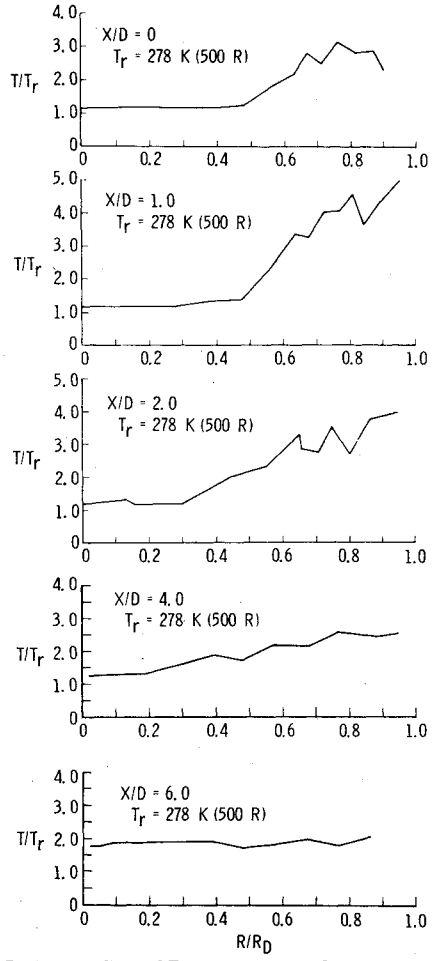


**Fig. 16 Radial profiles of Raman-measured mean temperatures.**

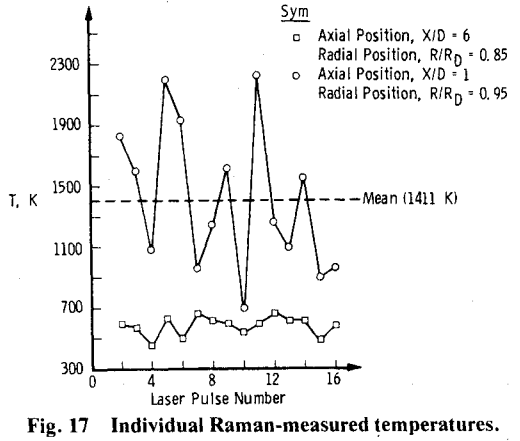


**Fig. 17 Individual Raman-measured temperatures.**

3) The maximum value of the turbulence intensity referenced to the jet exit mean velocity is about the same for the reacting and nonreacting cases, approximately 0.25. However, the location of the maximum turbulence intensity is reached closer to the primary nozzle in the nonreacting case because in each case the maximum turbulence location occurs near the midpoint of the length of the mixing zone, which extends farther downstream with chemical reaction. The magnitude of the radial velocity standard deviation is much greater than the mean radial velocity at nearly every point in the flowfield.

4) The hydrogen mass fraction, velocity, and turbulence intensity profiles indicate that counterstream turbulent diffusion dilutes the secondary hydrogen stream back close to the nozzle exit plane.

5) The extremely large temporal temperature fluctuations in the reacting flow as shown by the laser Raman temperature data indicate that in future turbulent combustion applications a data sample of at least 150 laser pulses per data point is required to provide data with a reasonably statistical confidence in mean values. Even larger sample sets would be required to assure confidence in measured variances. The large temporal fluctuations clearly indicate the requirement that any physically perceptive prediction technique must account for the huge fluctuations in temperature and concentration.

## Acknowledgments

The research reported herein was performed by the Arnold Engineering Development Center, Air Force Systems Command. The sponsor of the effort was the Air Force Office of Scientific Research under the guidance of B.T. Wolfson, Contract Monitor. Work and analysis for this research was done by personnel of ARO, Inc., a Sverdrup Corporation company, operating contractor of AEDC. Further reproduction is authorized to satisfy needs of the U.S. Government.

## References

[1] Smith, G.D. and Giel, T.V., "An Experimental Investigation of Reactive, Turbulent, Recirculating Jet Mixing," AEDC-TR-79-79 (ADA084546), May 1980.

[2] Schulz, R.J., "An Investigation of Ducted, Two-Stream, Variable Density, Turbulent Jet Mixing with Recirculation," AEDC-TR-76-152, AFOSR-TR-76-1087 (ADA034537), Jan. 1977.

[3] Chriss, D.E., "An Experimental Investigation of Ducted, Reactive Turbulent Jet Mixing with Recirculation," AEDC-TR-77-56, AFOSR-TR-77-0749 (ADA044110), Sept. 1977.

[4] Rhodes, R.P., "Probing Techniques for Use in High Temperature Reacting Flows," AEDC-TR-68-44 (AD829143), March 1968.

[5] Verdin, A., *Gas Analysis Instrumentation*, John Wiley & Sons, New York, 1973.

[6] Brewer, L.E. and Limbaugh, C.C., "Infrared Band Model Technique for Combustion Diagnostics," *Applied Optics*, Vol. 11, May 1972, pp. 1200-1204.

[7] Williams, W.D., Powell, H. M., Price, L. L., and Smith, G.D., "Laser-Raman Measurements in a Ducted, Two-Stream, Subsonic $H_2$/Air Combustion Flow," AEDC-TR-79-74 (ADA078112), Dec. 1979.

[8] Bendat, J.S. and Piersol, A.G., *Measurement and Analysis of Random Data*, John Wiley & Sons, New York, 1966.

[9] Barnett, D.O. and Giel, T.V., "Application of a Two-Component Bragg Diffracted Laser Velocimeter to Turbulence Measurements in a Subsonic Jet," AEDC-TR 76-36 (ADA025355), May 1976.

[10] Barnett, D.O. and Giel, T.V., "Laser Velocimeter Measurements in Moderately Heated Jet Flows," AEDC-TR-76-156 (ADA038283), April 1977.

[11] Rhodes, R.P., Harsha, P.T., and Peters, C.E., "Turbulent Kinetic Energy Analyses of Hydrogen-Air Diffusion Flames," *Acta Astronautica*, Vol. I, March-April 1974, pp. 443-470.